Harmel, T.; Agagliate, J.; Hieronymi, M.; Gernez, P.:
Two-term Reynolds–McCormick phase function parameterization better describes light scattering by microalgae and mineral hydrosols.
In: Optics Letters. Vol. 46 (2021) 8, 1860 - 1863.

First published online by OSA: 08.04.2021

https://dx.doi.org/10.1364/OL.420344

Two-term Reynolds–McCormick phase function parameterization better describes light scattering by microalgae and mineral hydrosols

Tristan Harmel,[1,2,*] Jacopo Agagliate,[3] Martin Hieronymi,[3] and Pierre Gernez[4]

[1]*Géosciences Environnement Toulouse (Centre National de la Recherche Scientifique—CNRS, Institut de Recherche pour le Développement—IRD, Université Paul Sabatier—UPS), Toulouse, 31400, France*

[2]*TH-Consulting, Nice, 06200, France*

[3]*Institute of Coastal Ocean Dynamics, Helmholtz-Zentrum Geesthacht (HZG), 21502 Geesthacht, Germany*

[4]*Université de Nantes, Mer Molécules Santé (MMS), Nantes, France*

**Corresponding author: tristan.harmel@get.omp.eu*

The presence of hydrosols, taken as suspension of micro- or macroscopic material in water, strongly alters light propagation and thus the radiance distribution within a natural or artificial water volume. Understanding of hydrosols' impacts on light propagation is limited by our ability to accurately handle the angular scattering phase function inherent to complex material such as suspended sediments or living cells. Based on actual quality-controlled measurements of sediments and microalgae, this Letter demonstrates the superiority of a two-term five-parameter empirical phase function as recently proposed for scattering by nanoparticle layers [Nanoscale 11, 7404 (2019)]. The use of such phase function parameterizations presents new potentialities for various radiative transfer and remote sensing applications related to an aquatic environment.

The presence of small particles in suspension in a water volume, also called hydrosols, deeply modifies and alters light propagation through or within a water body. In particular, the angular distribution of the light field is governed primarily by the interplay between directional shape of the scattering phase function and absorption [1,2]. In aquatic environment sciences, insights on the particles present, such as microalgae or suspended sediments, might be obtained through field measurements of the backscattering properties [3,4]. Similarly, exploitation of field or satellite measurements of the water-leaving radiance requires accurate radiative transfer modeling of the atmosphere–water system [5]. In oceanography, full understanding of directional scattering properties of phytoplankton is still needed to reconcile measurements obtained from distinct optical setups [6,7]. In studies involving cultured phytoplankton or related industrial applications, refined p arameterization o f t he scattering phase function of hydrosols is one of the basic requirements for engineering efforts to optimize photobioreactors [8]. Indeed, many fields, from Earth observation to industrial biomass production, are still impeded by flaws in our understanding and handling of the directional scattering properties of complex material such as heterogeneous compounds or living cells [9].

Hydrosols are represented by a large range of compounds of different sizes, shapes, roughnesses, and internal structures. For instance, suspended sediments exhibit a very wide range of mineralogical properties including complex microstructures or grain inclusions from natural or anthropogenic sources [10]. On the other hand, the internal structure of microalgae, or aquatic bacteria, consists of distinct organelles with highly variable shapes, thicknesses, and refractive indices, and adding to the structural complexity, those organelles are subdivided into smaller constituents with various optical properties [11]. A mixture of microbial, organic, and mineral particles might also be assembled into flocs as a particularly complex matrix [12]. In addition, environmental conditions (e.g., illumination, biogeochemistry, hydrodynamics, and shear flow) can produce rapid changes in the structure and orientation of microbial hydrosols [13,14].

Due to the highly diverse nature of hydrosols, two complementary approaches can be followed to accurately describe their inherent scattering phase function. First, the microphysical parameters describing the complex structure of a given hydrosol have to be reduced to a certain amount to appropriately simulate the scattering properties of a realistic ensemble of hydrosols through theoretical computations, e.g., [15–17]. The other approach is to use analytical approximation (also called empirical expression) of the phase function fitted on actual multi-angular scattering measurements (see Chapter 4 of [18] for a review of empirical expressions).

Historically, the phase function parameterization was developed for astronomical purposes with the Henyey–Greenstein (HG) model [19], which is a function of the asymmetry parameter. But it appeared that this single-term analytical function was unable to reproduce the glory observed in the backscattering angles of planetary atmospheres [20]. The superposition of

two single-term phase functions was then introduced to more accurately simulate this feature [21,22].

Two-term phase function parameterization was already proposed to improve the representativeness of the HG model for seawater constituents [23]. A recent study demonstrated the effectiveness of using two-term phase functions to represent scattering by layers containing colloidal nanospheres [24]. Here, we evaluate the performances of those models to fit actual measurements obtained for various mono-specific microalgae and mineral hydrosols.

One of the most common empirical phase functions used for aquatic studies was proposed by Fournier and Forand (FF) [25], which is a single-term phase function with two fitting parameters. Assuming homogeneous spheres with size following a power law, the FF phase function, p_{FF}, was formulated as a function of the bulk refractive index of hydrosols relative to surrounding water, n, and the slope, m, of a power law describing the particulate size distribution [18,25]:

$$p_{\mathrm{FF}}(\theta, n, m) = \frac{\left(v(1-\delta) - (1-\delta^v) + \frac{4}{u^2}[\delta(1-\delta^v) - v(1-\delta)]\right)}{4\pi(1-\delta)^2\delta^v} - \frac{1-\delta_\pi^v}{16\pi(1-\delta_\pi)\delta_\pi^v}(3\cos^2\theta - 1), \quad \textbf{(1)}$$

with the scattering angle θ and

$$v = \frac{3-m}{2}, \quad \delta = \frac{4}{3}\left(\frac{\sin(\theta/2)}{n-1}\right)^2, \quad \delta_\pi = \delta(\theta=\pi). \quad \textbf{(2)}$$

Another empirical phase function was proposed by Reynolds and McCormick (RM) as a generalization of the HG model for highly anisotropic scatterers [26]. The analytic form of the RM function is based on two fitting parameters g and α:

$$p_{\mathrm{RM}}(\theta, g, \alpha) = \frac{\alpha g(1-g^2)^{2\alpha}}{\pi((1+g)^{2\alpha} - (1-g)^{2\alpha})(1+g^2-2g\cos\theta)^{\alpha+1}}. \quad \textbf{(3)}$$

Note that the HG phase function [19] is a specific case of the RM phase function of Eq. (3) when $\alpha = 0.5$. Only in this case is the parameter g given directly as the asymmetry parameter, $\langle\cos\theta\rangle$ (also called *mean cosine*), associated with the phase function. In the RM model, the asymmetry parameter can be analytically formulated as a function of g and α (see [26] for details).

The two-term phase functions are simply based on the above expressions by introducing a mixing parameter γ (between zero and one). The two-term FF (TTFF) is given by

$$p_{\mathrm{TTFF}}(\theta, n_1, m_1, n_2, m_2, \gamma) = \gamma\, p_{\mathrm{FF}}(\theta, n_1, m_1) + (1-\gamma)\, p_{\mathrm{FF}}(\theta, n_2, m_2). \quad \textbf{(4)}$$

The two-term RM (TTRM) follows the same definition:

$$p_{\mathrm{TTRM}}(\theta, g_1, \alpha_1, g_2, \alpha_2, \gamma) = \gamma\, p_{\mathrm{RM}}(\theta, g_1, \alpha_1) + (1-\gamma)\, p_{\mathrm{RM}}(\theta, g_2, \alpha_2). \quad \textbf{(5)}$$

The two-term models allow using a greater number of fitting parameters, which increases the degree of freedom and therefore the flexibility of the fitting procedure.

The efficiency of each of the four models has to be evaluated against quality-controlled data of the angular scattering of actual hydrosols. Accurate measurements of the hydrosol phase function are still challenging despite long-term efforts to build novel instrumentation (see [27–32]). Furthermore, published measurements over a wide range of scattering angles are scarce. In this study, we investigate two different datasets—first, the widely used measurements made in the early 1970s by Petzold [27] for natural sea water samples at 514 nm with a bandwidth of 75 nm. It is worth noting that those measurements were performed with two different instruments, one for three forward angles (0.17°, 0.34°, 0.57°) and the other for angles between 10° and 170°. Unfortunately, very large uncertainty is attached to the forward measurements [2]. Consequently, those three angular measurements were removed from the fitting procedure since they might strongly bias the overall results. The second dataset was obtained from a laboratory experiment [33] encompassing five microalgae species and one dust sample (see [33] for complete description). The originality of the latter dataset comes from the coincident use of three conceptually different instruments: I-VSF [29], LISST-VSF [34], and POLVSM [30]. Note that only the multispectral data (I-VSF, POLVSM) were used for fitting purposes.

The representativeness of the single-term and two-term models was evaluated based on nonlinear fitting. The fitting procedure is based on the Levenberg–Marquardt algorithm [35] with bound constraints through the *trust region reflective* approach [36] (see Supplement 1). Due to the very large amplitudes of typical hydrosol phase functions (> five orders of magnitude), the cost function to minimize, Ψ, was expressed in the logarithmic space:

$$\Psi(\boldsymbol{x}) = \frac{1}{2}\sum_i^{N_{\mathrm{obs}}} \| \log p^{\mathrm{meas}}(\theta_i) - \log p^{\mathrm{model}}(\theta_i, \boldsymbol{x}) \|^2, \quad \textbf{(6)}$$

where N_{obs} is the number of angular measurements of the phase function, and $\mathbf{x}$ is the vector of unknown parameters, which is of dimension N_{param} equal to two and five for the single-term and two-term models, respectively. Note that bounds constraint was applied to $\mathbf{x}$ in accordance with the feasible values of each model parameter.

The results of the fitting procedure are illustrated in Fig. 1 for the Petzold dataset and some of the sampled hydrosols measured in laboratory [33]; results for all samples are provided in Supplement 1. The performances of the fit are given in Fig. 2 as the reduced chi-squared coefficient, $\chi_v^2 = 2\Psi/(N_{\mathrm{obs}} - N_{\mathrm{param}})$, i.e., the lower the χ^2, the better the model reproduces the angular behavior.

The TTRM model outperforms the other models over the full range of scattering angles (Figs. 1 and 2). In the case of the hydrosols analyzed here, the residuals between measurements and TTRM fitting can be one order of magnitude lower than those obtained from the FF model except for the *D. salina* species for which the four models led to virtually similar performances. Regarding the application to the Petzold phase functions, TTRM provides the best fit for clear and coastal samples, whereas TTRM and FF offer similar performances for the turbid case. Note that similar results were obtained when

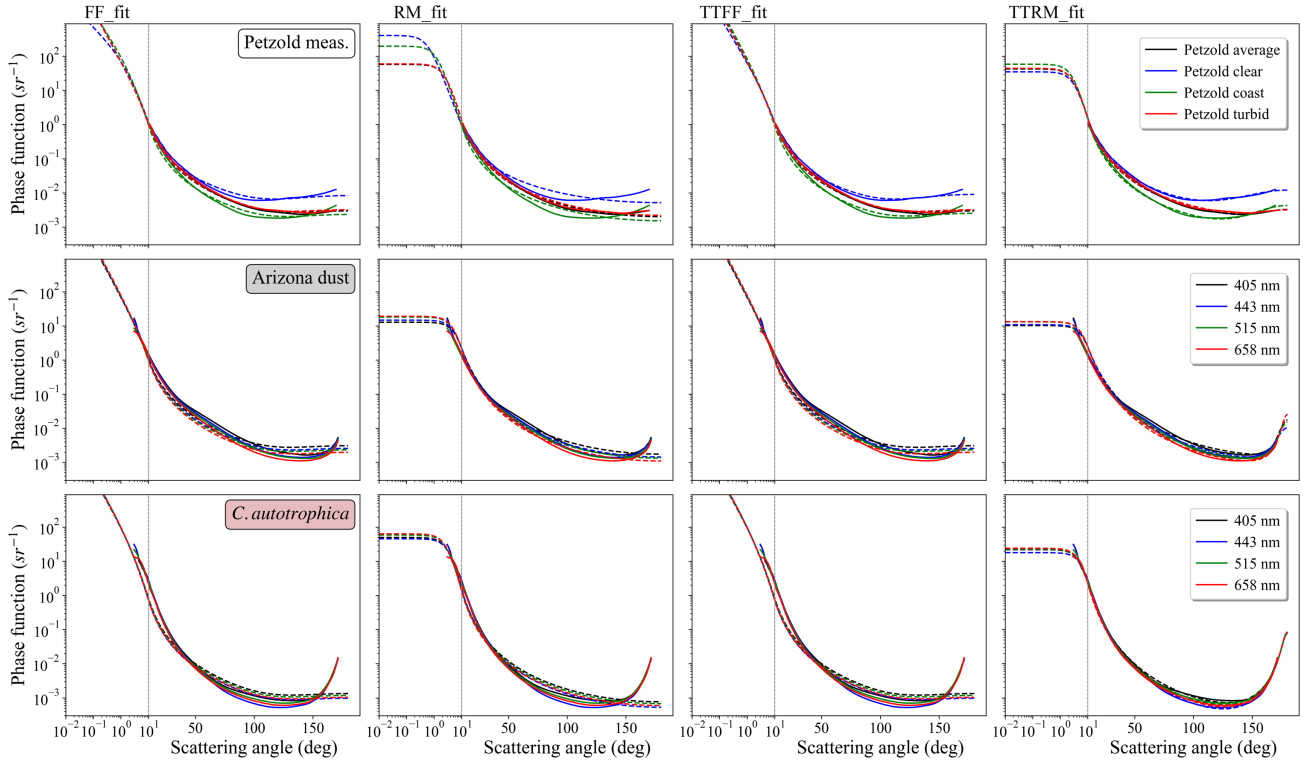

Fig. 1. Results of the fit for four phase function empirical models (columns) applied to the Petzold dataset and laboratory samples (rows) at several wavelengths for Arizona dust and two different microalgae species. The results obtained for all the analyzed samples are given in Supplement 1. Continuous lines represent measurement data and dashed lines the fitting results; colors indicate the water type for the Petzold dataset and wavelengths for which measurements were performed (rows 2–4). Note that x axes are given in logarithmic scale for scattering angles smaller than 10° and in linear scale afterward.

considering a restricted scattering angle range: the TTRM still outperforms the other models even when angles larger than 140° are ignored. This result implies that the TTRM could provide a new means to extrapolate phase function measurements when instrumentation is limited in the backward direction [37].

The five fitting parameters of the TTRM model are given in Fig. 3. The mixing coefficient, γ, is very close to one for all samples. This means that the forward scattering is well represented

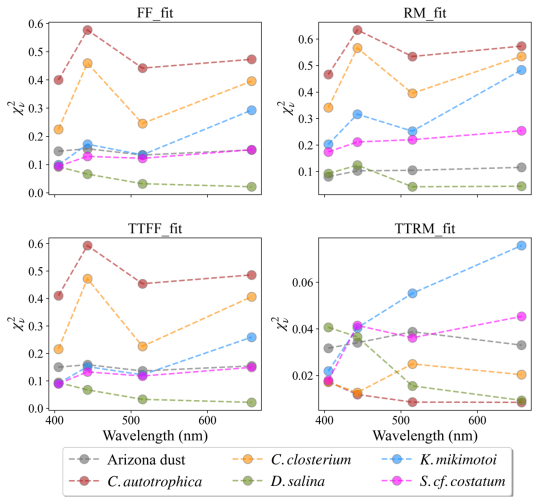

Fig. 2. Spectral performances in terms of reduced chi-square of the fitting models applied to measurements of Fig. 1 over the 3°–173° angle range.

Table 1. Fitting Parameters of TTRM Retrieved for Petzold Measurements Along with Backscattering Ratio, $\tilde{b}_b$, and Asymmetry Parameter, $\langle \cos\theta \rangle$

	γ	g_1	g_2	α_1	α_2	$\tilde{b}_b$	$\langle \cos\theta \rangle$
Average	0.999	0.944	−0.453	0.43	2.5	0.019	0.921
Clear	0.978	0.944	−0.267	0.35	2.5	0.044	0.858
Coast	0.996	0.947	−0.378	0.53	2.5	0.013	0.944
Turbid	0.999	0.947	−0.394	0.40	2.5	0.020	0.917

by the single-term RM model. Nevertheless, the backward features are captured only by addition of the second term in the TTRM model. Parameters g_1 and g_2, which control the curvature in forward and backward directions, respectively, exhibit a certain variability between the different samples. Those two parameters could provide a potential way of discriminating between algae species, for example. Note also that the retrieved α parameters significantly depart from the 0.5 value considered in the HG model.

The fitting model enables to extrapolate the phase function measurements over the full range of scattering angles. Based on the TTRM model, the spectral backscattering ratio and asymmetry parameters were computed for all the samples (Table 1 and Fig. 3). Those values show slight spectral dependence for most of the samples except that corresponding to the *D. salina* species. However, interpretation of those spectral variations should be done on a greater amount of measurements and if possible in a hyperspectral manner. Nonetheless, the

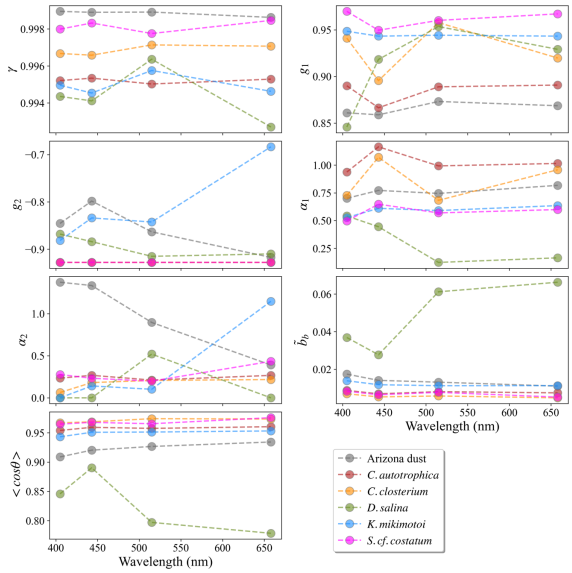

Fig. 3. Fitting and optical parameters retrieved from TTRM applied to dust and microalgae samples.

fitting p rocedure w ith T TRM m ay h elp d ata h andling and interpretation.

As argued by Wang *et al*. [24], the TTRM model provides sufficient mathematical flexibility to represent both single and multiple scattering features (or independent and dependent scattering [38]) that might occur within complex hydrosol compounds. Furthermore, such a parametric model offers a practical tool for implementation in radiative transfer numerical codes. On the other hand, the TTRM model could be used to better represent and understand field o r l aboratory measurements. Based on this model, important optical parameters can be accurately calculated such as the asymmetry parameter, the backscattering-to-scattering ratio, or even the backscatter coefficient.

In summary, we demonstrated that the TTRM model provides significantly h igher p erformances t o fi t ph ase functions of actual living or mineral hydrosols than the widely used single-term parametrizations. This TTRM model could be advantageously used in numerical radiative transfer simulation or the water-radiance analytical model [39]. This Letter focused purely on goodness-of-fit p arameters w hen fitting hydrosol phase functions from 3° to 173°. Future work will also have to consider the weight of other finer details, e.g., the stark differences between models in scattering behavior at forward angles (<3°). Nevertheless, a foreseeable application of the TTRM model will be to further elucidate relationships between the fitting p arameters a nd t he k ey p arameters controlling bio-optical or mineralogical properties of hydrosols.

Funding. Centre National d'Etudes Spatiales (TOSCA - LASHA, TOSCA - OBS2CO).

Acknowledgment. The authors are thankful to Rüdiger Röttgers for helping discussions as well as to the three reviewers.

Disclosures. The authors declare no conflicts of interest.

Data Availability. Data underlying the results presented in this paper are not publicly available at this time but may be obtained from the authors upon reasonable request. See Code 1 [40] for the phase functions Python package.

REFERENCES

1. H. C. van de Hulst, *Light Scattering by Small Particles* (Dover/Wiley, 1981).
2. C. D. Mobley, *Light and Water* (Academic, 1994).
3. F. Chai, K. S. Johnson, H. Claustre, X. Xing, Y. Wang, E. Boss, S. Riser, K. Fennel, O. Schofield, and A. Sutton, Nat. Rev. Earth Environ. **1**, 315 (2020).
4. C. B. Mouw, S. Greb, D. Aurin, P. M. DiGiacomo, Z. Lee, M. Twardowski, C. Binding, C. Hu, R. Ma, T. Moore, W. Moses, and S. E. Craig, Remote Sens. Environ. **160**, 15 (2015).
5. J. Chowdhary, P. W. Zhai, E. Boss, H. Dierssen, R. Frouin, A. Ibrahim, Z. Lee, L. A. Remer, M. Twardowski, F. Xu, X. Zhang, M. Ottaviani, W. R. Espinosa, and D. Ramon, Front. Earth Sci. **7**, 100 (2019).
6. D. Stramski, E. Boss, D. Bogucki, and K. J. Voss, Prog. Oceanogr. **61**, 27 (2004).
7. E. Organelli, G. Dall'Olmo, R. J. W. Brewin, G. A. Tarran, E. Boss, and A. Bricaud, Nat. Commun. **9**, 5439 (2018).
8. J. Dauchet, J. F. Cornet, F. Gros, M. Roudet, and C. G. Dussap, *Advances in Chemical Engineering* (Academic, 2016), Vol. **48**, pp. 1–106.
9. A. Bhowmik and L. Pilon, J. Opt. Soc. Am. A **33**, 1495 (2016).
10. J. A. Brandon, W. Jones, and M. D. Ohman, Sci. Adv. **5**, eaax0587 (2019).
11. A. Lehmuskero, M. Skogen Chauton, and T. Boström, Prog. Oceanogr. **168**, 43 (2018).
12. I. G. Droppo, Hydrol. Process. **15**, 1551 (2001).
13. C. Poulin, X. Zhang, P. Yang, and Y. Huot, J. Quant. Spectrosc. Radiat. Transf. **217**, 288 (2018).
14. Marcos, J. R. Seymour, M. Luhar, W. M. Durham, J. G. Mitchell, A. Macke, and R. Stocker, Proc. Natl. Acad. Sci. USA **108**, 3860 (2011).
15. M. A. Yurkin and A. G. Hoekstra, J. Quant. Spectrosc. Radiat. Transf. **112**, 2234 (2011).
16. B. Sun, G. W. Kattawar, P. Yang, M. S. Twardowski, and J. M. Sullivan, J. Quant. Spectrosc. Radiat. Transf. **178**, 390 (2016).
17. T. Wriedt, J. Quant. Spectrosc. Radiat. Transf. **110**, 833 (2009).
18. M. Jonasz and G. R. Fournier, *Light Scattering by Particles in Water* (Elsevier, 2007).
19. L. G. Henyey and J. L. Greenstein, Astrophys. J. **93**, 70 (1941).
20. L. P. Whitehill and J. E. Hansen, Icarus **20**, 146 (1973).
21. W. M. Irvine, J. Opt. Soc. Am. **55**, 16 (1965).
22. G. W. Kattawar, J. Quant. Spectrosc. Radiat. Transf. **15**, 839 (1975).
23. V. I. Haltrin, Appl. Opt. **41**, 1022 (2002).
24. J. Wang, C. Xu, A. M. Nilsson, D. L. A. Fernandes, and G. A. Niklasson, Nanoscale **11**, 7404 (2019).
25. G. R. Fournier and J. L. Forand, Proc. SPIE **2258**, 194 (1994).
26. L. O. Reynolds and N. J. McCormick, J. Opt. Soc. Am. **70**, 1206 (1980).
27. T. J. Petzold, Volume scattering functions for selected ocean waters (DTIC Document, 1972).
28. M. E. Lee and M. R. Lewis, J. Atmos. Ocean. Technol. **20**, 563 (2003).
29. H. Tan, R. Doerffer, T. Oishi, and A. Tanaka, Opt. Express **21**, 18697 (2013).
30. M. Chami, A. Thirouard, and T. Harmel, Opt. Express **22**, 26403 (2014).
31. G. Kullenberg, Opt. Asp. Oceanogr. **25**, 354 (1974).
32. J. E. Tyler and W. H. Richardson, J. Opt. Soc. Am. **48**, 354 (1958).
33. T. Harmel, M. Hieronymi, W. Slade, R. Röttgers, F. Roullier, and M. Chami, Opt. Express **24**, A234 (2016).
34. W. H. Slade, Y. C. Agrawal, and O. A. Mikkelsen, in *Oceans* (2013), pp. 23–27.
35. J. J. Moré, *The Levenberg-Marquardt Algorithm: Implementation and Theory* (Springer, 1978), pp. 105–116.
36. M. A. Branch, T. F. Coleman, and Y. Li, SIAM J. Sci. Comput. **21**, 1 (1999).
37. J. M. Sullivan and M. S. Twardowski, Appl. Opt. **48**, 6811 (2009).
38. T. Galy, D. Huang, and L. Pilon, J. Quant. Spectrosc. Radiat. Transf. **246**, 106924 (2020).
39. M. Twardowski and A. Tonizzo, Appl. Sci. **8**, 2684 (2018).
40. T. Harmel, "Tools for scattering phase functions," GitHub (2021) https://github.com/Tristanovsk/pffit